

Corneal Decellularization: A Method of Recycling Unsuitable Donor Tissue for Clinical Translation?

Samantha L. Wilson, Laura E. Sidney, Siobhán E. Dunphy, Harminder S. Dua and Andrew Hopkinson

Academic Ophthalmology, Division of Clinical Neuroscience, Queen's Medical Centre Campus, University of Nottingham, Nottingham, UK

ABSTRACT

Background: There is a clinical need for biomimetic corneas that are as effective, preferably superior, to cadaveric donor tissue. Decellularized tissues are advantageous compared to synthetic or semi-synthetic engineered tissues in that the native matrix ultrastructure and intrinsic biological cues including growth factors, cytokines and glycosaminoglycans may be retained. However, there is currently no reliable, standardized human corneal decellularization protocol.

Methods: Corneal eye-bank tissue unsuitable for transplantation was utilized to systematically compare commonly used decellularization protocols. Hypertonic sodium chloride; an ionic reagent, sodium dodecyl sulphate; a non-ionic detergent, tert-octylphenol polyoxyethylene (Triton-X); enzymatic disaggregation using Dispase; mechanical agitation; and the use of nucleases were investigated. Decellularization efficacy, specifically for human corneal tissue, was extensively evaluated. Removal of detectable cellular material was evidenced by histological, immunofluorescence and biochemical assays. Preservation of macroscopic tissue transparency and light transmittance was evaluated. Retention of corneal architecture, collagen and glycosaminoglycans was assessed via histological, immunofluorescence and quantitative analysis. Biocompatibility of the resulting scaffolds was assessed using cell proliferation assays.

Results: None of the decellularization protocols investigated successfully removed 100% of cellular components. The techniques with the least residual cellular material were most structurally compromised. Biochemical analysis of glycosaminoglycans demonstrated the stripping effects of the decellularization procedures.

Conclusion: The ability to utilize, reprocess and regenerate tissues deemed “unsuitable” for transplantation allows us to salvage valuable tissue. Reprocessing the tissue has the potential to have a considerable impact on addressing the problems associated with cadaveric donor shortage. Patients would directly benefit by accessing greater numbers of corneal grafts and health authorities would fulfill their responsibility for the delivery of effective corneal reconstruction to alleviate corneal blindness. However, in order to progress, we may need to take a step back to establish a “decellularization” criterion; which should balance effective removal of immune reactive material with maintenance of tissue functionality.

Keywords: Biocompatibility, collagen, corneal decellularization, glycosaminoglycans, residual cellular material, stromal transparency

INTRODUCTION

There are approximately 1.5 million cases of corneal blindness diagnosed annually and 10 million untreated patients worldwide.^{1–6} Presently, there are

insufficient numbers of suitable corneas for allografting to meet demand, particularly in Africa and Asia predominantly due to cultural, religious, logistical and technical issues.^{7,8} An ageing population, increasing worldwide trends for refractive surgery, and the

Received 25 February 2015; revised 26 May 2015; accepted 7 June 2015; published online 21 September 2015

© Samantha L. Wilson, Laura E. Sidney, Siobhán E. Dunphy, Harminder S. Dua and Andrew Hopkinson.

Correspondence: Samantha L. Wilson, Academic Ophthalmology, Division of Clinical Neuroscience, University of Nottingham, Queens Medical Centre campus, Nottingham, NG7 2UH, UK. E-mail: Samantha.wilson@nottingham.ac.uk

Color versions of one or more of the figures in the article can be found online at www.tandfonline.com/icey.

relative short shelf-life of suitable corneas⁹ further compound the issue. Where supply is not an issue, the quality of cadaveric tissue is variable, and despite its "immune privileged" status,^{10–12} 1 in 6 full-thickness allografts experience some degree of rejection,¹³ usually caused by immunological responses to epithelial or endothelial antigens. This highlights the compelling need to develop procedures to manufacture reliable, reproducible biomimetic corneas as effective, preferably superior to cadaveric tissue for clinical translation.

Despite huge advances in tissue engineering, there is yet to be a successful biological or synthetic engineered corneal tissue in routine clinical practice. Often, they do not meet the clinical demand for long-term biocompatibility and regenerative capacity, transparency and sufficient mechanical strength.¹⁴ Fundamental challenges include: replication of the unique tissue structure, complete with intrinsic biological and topographical cues and the maintenance of healthy corneal cells. The lack of nanoscale tissue architecture in tissue engineered constructs often results in a construct with compromised biomechanical properties, a lack of tensile strength, tissue curvature, reduced optical properties and ultimately rejection following implantation.

In western countries, such as the UK, many harvested corneas are rejected for transplantation as they fail to meet the biological screening criteria (44%, 1846 corneas¹⁵). In most cases, the tissues are structurally intact, so the ability to reprocess these tissues as a clinically relevant product could have considerable impact on addressing shortages. Presently, few studies investigate the use of human tissue,^{16,17} and there is currently no standardized decellularization protocol specifically for human corneal tissue. Comparatively, xenogeneic matrices have been comprehensively investigated.^{8,18–26} Unfortunately, interspecies differences are a prevalent problem leading to graft failure.²⁷ Furthermore, xenogeneic materials face many more immunological and regulatory barriers compared to human tissue. Thus, utilizing human tissue may be a simpler solution. To realize this, the development of appropriate decellularization methods is of utmost importance.

Commonly employed methods of decellularization include the use of detergents, including ionic, non-ionic and zwitter-ionic detergents and hypertonic solutions.^{14,22,28} Extensive reviews of decellularization methods can be found elsewhere.^{29–32} Extensive use of decellularizing reagents coupled with varying, often laborious, protocols make evaluating existing decellularization techniques and their applicability to human corneal applications, difficult to compare. Furthermore, due to cost and methodological complexity implications, many techniques are not up-scalable from a manufacturing point of view, a factor which needs to be considered when designing

clinically viable tissues. In addition, published corneal decellularization protocols often lack full characterization of the decellularized tissue, relying largely on qualitative data, resulting in misleading and/or conflicting results.

The aim of this article is to provide a systematic comparison of commonly used decellularization methods including: hypertonic sodium chloride (NaCl); an ionic reagent, sodium dodecyl sulphate (SDS); a non-ionic detergent, tert-octylphenol polyoxyethylene (Triton-X); enzymatic disaggregation using Dispase, mechanical agitation; and nucleases. Human corneas are extensively evaluated using both qualitative and quantitative analysis to ascertain if an appropriate balance between removal of cellular material while maintaining the corneal structure and important biological cues is achievable.

MATERIALS AND METHODS

Human Cornea Decellularization

All reagents were purchased from Sigma-Aldrich, Poole, UK, unless otherwise stated. Corneas unsuitable for transplantation were utilized in this study. Often the corneas have been stored for periods exceeding 2 months. Human tissue use was approved by the local ethics research committee (NRES Committee East Midlands-Nottingham 1, 07/H0403/140), in accordance with the tenants of the declaration of Helsinki, following consent from the donors or their relatives. Excess scleral tissue was removed aseptically and the corneas were washed in 10 mL phosphate buffered saline (PBS, 3 × 5 min) at room temperature (RT).

The corneas were initially decellularized using 10 mL of the following reagents; (i) hypertonic solution, 1.5 M NaCl in PBS; (ii) ionic-detergent, 0.5% *w/v* SDS in PBS (Amersham BioScience, Bucks, UK); or (iii) non-ionic detergent, 1% *w/v* Triton-X100 in PBS. All decellularization solutions contained 1× complete protease inhibitors (Roche, Hertfordshire, UK) used according to the manufacturer's instructions. All corneas were incubated at 4°C with agitation for 24 h (SRT6 roller mixer, Stuart, SLS, Yorkshire, UK) followed by washing in 10 mL PBS (2 × 24 h with agitation). Three "control" corneas were investigated: (i) Stromal controls were prepared by overnight treatment at 4°C with 2.4 U/mL Dispase II (CellnTec, Bern, Switzerland) before removing the epithelium and endothelium using sharp-point forceps; (ii) agitated controls were subjected to mechanical agitation in 10 mL PBS; (iii) complete controls were simply stored under 10 mL PBS at RT (changed daily) for the duration of the experiment. All the aforementioned conditions were repeated, with an additional nuclease treatment as previously

described.¹⁶ Briefly, corneas were treated with 10 mL 5 U/mL DNase and 5 U/mL RNase for 48 h under agitation (2 × 24 h). The corneas were then washed in 10 mL PBS for 72 h, with agitation, with PBS changed every 24 h.

Macroscopic Evaluation and Light Transmittance

Corneal tissues were appraised macroscopically pre- and post-treatment. Digital images were recorded (Samsung SM-G357FZ). Light transmittance was evaluated using a fluorescent spectrophotometer (Tecan Infinite[®] 200 PRO). Absorbance was measured at 480 nm and 21 readings were taken across each cornea ($n=5$); a mean value was calculated accounting for tissue heterogeneity. Data were analyzed as a mean percentage loss of transparency compared to the tissue transparency pre-treatment.

Histology and Immunohistochemistry

Harris Hematoxylin (VWR International, Germany) and 1% eosin (RAL Diagnostics, France) was used to evaluate tissue architecture. Samples were stained with 1% Alcian blue 8GX for 5 min followed by washing in diH₂O to visualize glycosaminoglycan (GAG) content. Samples were examined using an inverted microscope (Leica, DM-1RB, Leica, Milton Keynes, UK).

Rehydrated tissue sections were also subjected to blocking with bovine serum albumin (BSA, 1% *w/v* in PBS) for 60 min. BSA was removed before staining with either rabbit anti-collagen-I polyclonal antibody (Abcam, Cambridge, UK) to evaluate tissue architecture; or mouse anti-human keratan-sulfate monoclonal antibody (Clone: EFG-11 (1A3), AbD Serotec, Oxford, UK) to assess maintenance/disruption of keratan sulfate (1:200 dilution in 1% BSA) overnight at 4 °C. The samples were washed (3 × 5 min) in PBS. Alexa fluor 488 donkey anti-rabbit IgG or Alexa fluor 594 donkey anti-mouse IgG (Life Technologies, Paisley UK) were used to fluorescently label the samples (1:200 dilution in 1% BSA) for 1 h at RT. Collagen-I stained samples were counterstained with 4', 6-diamidino-2-phenylindole (DAPI) (1:500), and examined using an upright fluorescent microscope (Olympus BX51, Southend-on-Sea, UK).

DNA Quantification

Corneal tissues were processed for DNA extraction by desiccating the tissue (Christ-Alpha 1-4 LSC Freeze Dryer), and then recording the dry mass of each sample. DNA was extracted and purified using a

DNeasy Blood and Tissue Kit (Qiagen, Crawley, UK) according to the manufacturer's instructions. The resulting contaminant-free bound DNA was eluted into 20 µL buffer solution prior to spectroscopic analysis using a Quant-iT[™] PicoGreen[®] dsDNA Assay Kit (Molecular Probes, Cambridge, UK) according to the manufacturer's instructions. Fluorescence was measured at excitation wavelength of 480 nm and emission wavelength of 520 nm. Residual DNA was normalized to the dry weight of the tissue. Five corneas per treatment were analyzed, all measurements were performed in triplicate.

Collagen Quantification

The collagen content of decellularized corneas was determined using a Sircol[™] soluble collagen assay (Biocolor Ltd, Belfast, UK) according to the manufacturer's protocol. Corneas were desiccated and their dry weight recorded, prior to digestion for 16 days at RT in pepsin extraction reagent (10 mg/mL in 0.5 M acetic acid). Digested samples were added to 1 mL Sircol[™] dye reagent and mechanically agitated for 30 min, followed by centrifugation. The pellet was washed in 750 µL acid salt wash reagent prior to centrifugation. Alkali reagent (250 µL) released the collagen-bound dye into solution, 200 µL was added to individual wells of a clear 96-well plate (Nunc, ThermoScientific, Runcorn, UK). Absorbance was measured at wavelength 555 nm. Five corneas per treatment were analyzed. Collagen values were calculated by comparing the samples to a standard curve. Data is represented as a percentage of collagen per cornea dry weight. Non-nuclease treated corneas were omitted from these experiments.

Sulfated Glycosaminoglycan Quantification

The sulfated GAG (sGAG) content of decellularized corneas was determined using a 1,9-dimethyl methylene blue (DMMB) assay (Biocolor Ltd., Belfast, UK) according to the manufacturer's protocol. Corneas were desiccated and their mass recorded, prior to digestion for 3 h at 65 °C in papain extraction reagent (125 µg/mL papain in 0.2 M sodium phosphate buffer, 5 mM EDTA disodium salt, 10 mM cysteine hydrochloride, pH 6.4) as previously described.³³ Digested sample (16 µL in 84 µL RNase-free water) was added to 1 mL 1,9-DMMB and mechanically agitated for 30 min to form a precipitate sGAG-dye complex before being centrifuged. Five corneas per treatment were analyzed, all sample measurements were performed in duplicate. sGAG values were calculated by comparing the sample values to a standard curve. sGAG content was adjusted for dry weight and normalized for blank assay controls.

Scaffold Biocompatibility

Corneal stromal cells (CSC) were cultured in the presence of decellularized and control corneas. CSC were isolated from adult human corneal rims as previously described.³⁴ CSC were cultured in cell culture flasks containing M199 medium supplemented with 2% (*v/v*) heat-inactivated fetal bovine serum (Fisher Scientific, UK), 0.02 µg/mL gentamicin, 0.5 ng/mL amphotericin B (combination, Gibco, Invitrogen, Paisley, UK) and 1.59 mM L-glutamine. 0.1×10^6 third passage CSC per well were seeded into 12-well companion plates (BD, Falcon, Franklin Lakes, NJ) and cultured for 24 h under 1 mL media. Corneal tissues were aseptically dissected into small pieces and placed onto sterile 12-well cell culture insert dishes (pore size 0.4 µm; BD, Falcon) above the CSC. CSC were also cultured alone (cellular control), and control media collected.

Negative controls whereby 0.5% *w/v* SDS in media was added to the stromal cells were assessed.

Cell proliferation was assessed using a PrestoBlue™ cell viability assay (Molecular Probes, Invitrogen, UK) according to the manufacturer's instructions. Cell viability was assessed at 0, 3, 7, 10 and 14 days. Fluorescence was measured at an excitation wavelength of 560 nm and emission wavelength of 590 nm. Five corneas per treatment were analyzed, all measurements were performed in triplicate. Non-nuclease treated corneas were omitted from these experiments.

Statistical Analysis

Statistical analysis was performed using GraphPad Prism® software (GraphPad Software Inc., San Diego, CA). Data is represented as mean ± standard deviation. The statistical differences were evaluated by either one-way or two-way ANOVA, followed by Tukey's or Bonferroni's multiple comparisons tests. Statistical significance was indicated at four levels: * $p \leq 0.05$, ** $p \leq 0.01$, *** $p \leq 0.001$, **** $p \leq 0.0001$.

RESULTS

Corneal Transparency and Light Transmittance

Macroscopic tissue evaluation suggested that mechanical agitation and NaCl did not affect transparency (Figure 1Aix–x). Triton-X-treated corneas experienced some tissue clouding (Figure 1Axi), but stromal controls (Figure 1Aiii) and SDS corneas (Figure 1Axi) appeared the most cloudy/opaque following decellularization. Irrespective of the initial

decellularization treatment, all nuclease treated tissues were cloudy/opaque (Figure 1Axiii–xviii).

Spectroscopic analysis demonstrated no significant difference in transparency prior to decellularization (Figure 1B). Following decellularization, spectroscopic analysis validated macroscopic evaluations confirming that mechanical agitation and NaCl had no significant effect on transparency compared to the complete controls. Triton-X had no significant effect on transparency despite macroscopic evaluations indicating opacities. Stromal controls had significantly reduced transparency compared to agitated controls ($p \leq 0.05$), NaCl ($p \leq 0.05$) and Triton-X-treated corneas ($p \leq 0.05$). SDS-treated corneas had most significant loss of transparency compared to all other groups ($p \leq 0.001$).

Following nuclease treatment, all groups experienced a significant reduction in transparency ($p \leq 0.01$ for stromal controls and NaCl; $p \leq 0.05$ for agitated controls and Triton-X-treated corneas; $p \leq 0.001$ for SDS-treated corneas).

Collagen Structure and Integrity

Hematoxylin/eosin histological and collagen-I immunohistochemical staining revealed changes to the stromal architecture following decellularization (Figure 2Ai–iv and Bi–iv). All treatments disrupted the lamellae structure, particularly in the posterior stroma. SDS caused greatest disruption, demonstrated by increased interfibrillar spacing and tissue voids (Figure 2Av and Bv). Although disruption was observed in the stromal controls (Figure 2Bii), it was not to the extent of corneas treated with decellularizing reagents. Minimal disruption was observed in agitated controls (Figure 2Aiii and Biii), although the epithelium and endothelium were absent. The addition of nucleases caused subtle interfibrillar disruption (Figure 2Avii–xii and Bvii–xii), most apparent in stromal controls (Figure 2Bviii), agitated controls (Figure 2Bix) and SDS-treated corneas (Figure 2A xi and Bxi). Corneas were also dissected upon arrival into the laboratory (Fresh) and compared to the control tissues (Figure 2E). PBS had no apparent effect on the tissue structure.

Residual DNA Staining and Quantification

DAPI staining revealed that all initial decellularization treatments failed to eradicate nuclear material (Figure 3Ai–iv). Following nuclease treatment DAPI staining was significantly reduced (Figure 3Avii–xii); although still detectable in the complete control (Figure 3Avii), agitated control (Figure 3Axi) and NaCl-treated corneas (Figure 3Ax).

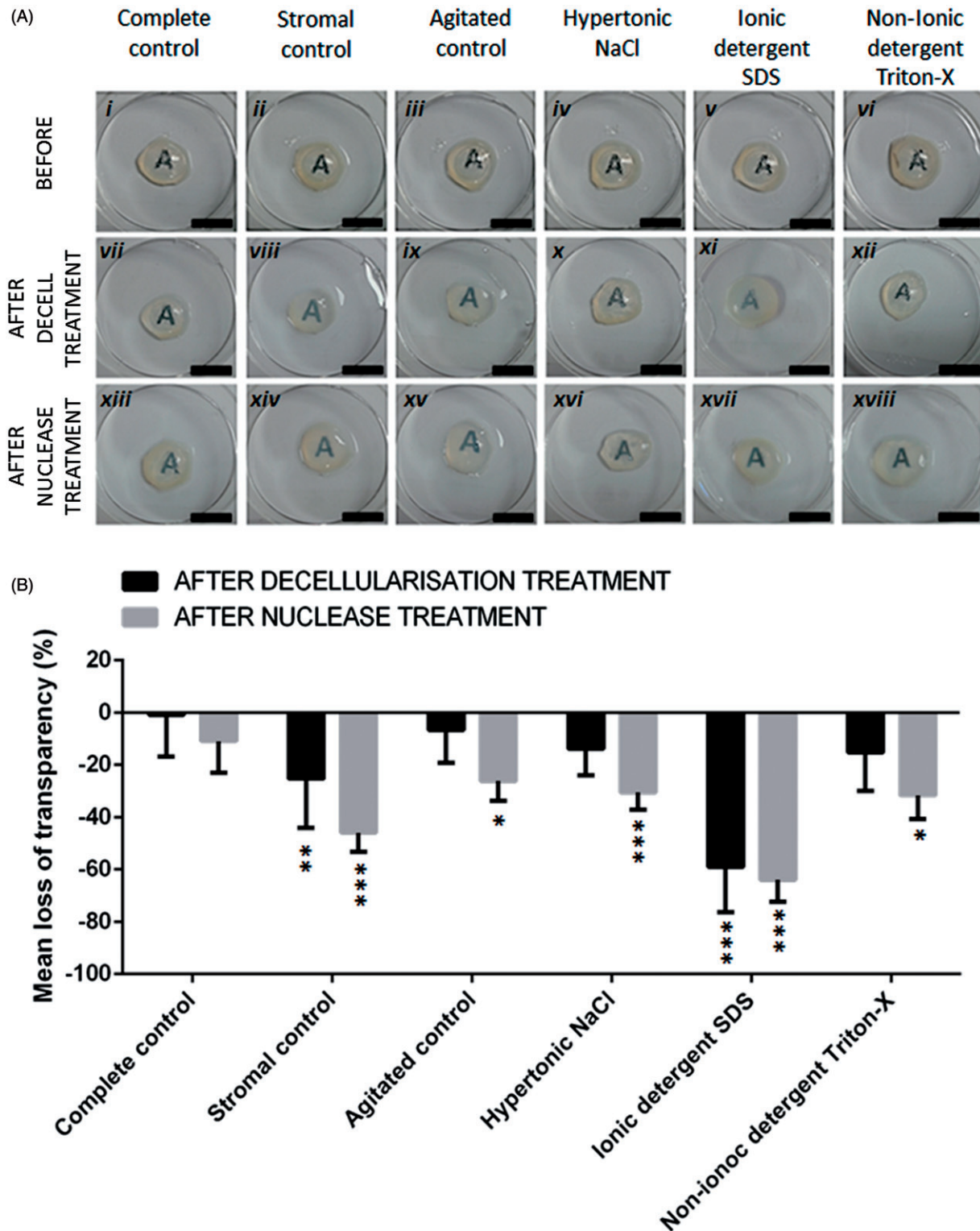


FIGURE 1 (A) Macroscopic evaluation of corneal tissue transparency following decellularization treatments and nuclease treatments, scale bar = 1 cm. (B) Quantitative analysis of loss of light transmittance following decellularization and nuclease treatments, $n = 5$. Data represented as the mean value \pm the calculated SD. * $p \leq 0.05$, ** $p \leq 0.01$, *** $p \leq 0.001$, when comparing the complete control corneas to decellularized tissues, stromal and agitated controls pre- and post-nuclease treatment.

PicoGreen[®] spectroscopic analysis was used to quantitatively evaluate residual DNA. All corneas demonstrated lower DNA content than the complete control (Figure 3B). SDS was most effective at removing DNA (approximately 56%) and was

significantly lower compared to all other control/treated corneas ($p \leq 0.05$). Triton-X removed approximately 23% and NaCl removed approximately 19% of DNA. Residual DNA in all control corneas was not significantly different from the complete controls.

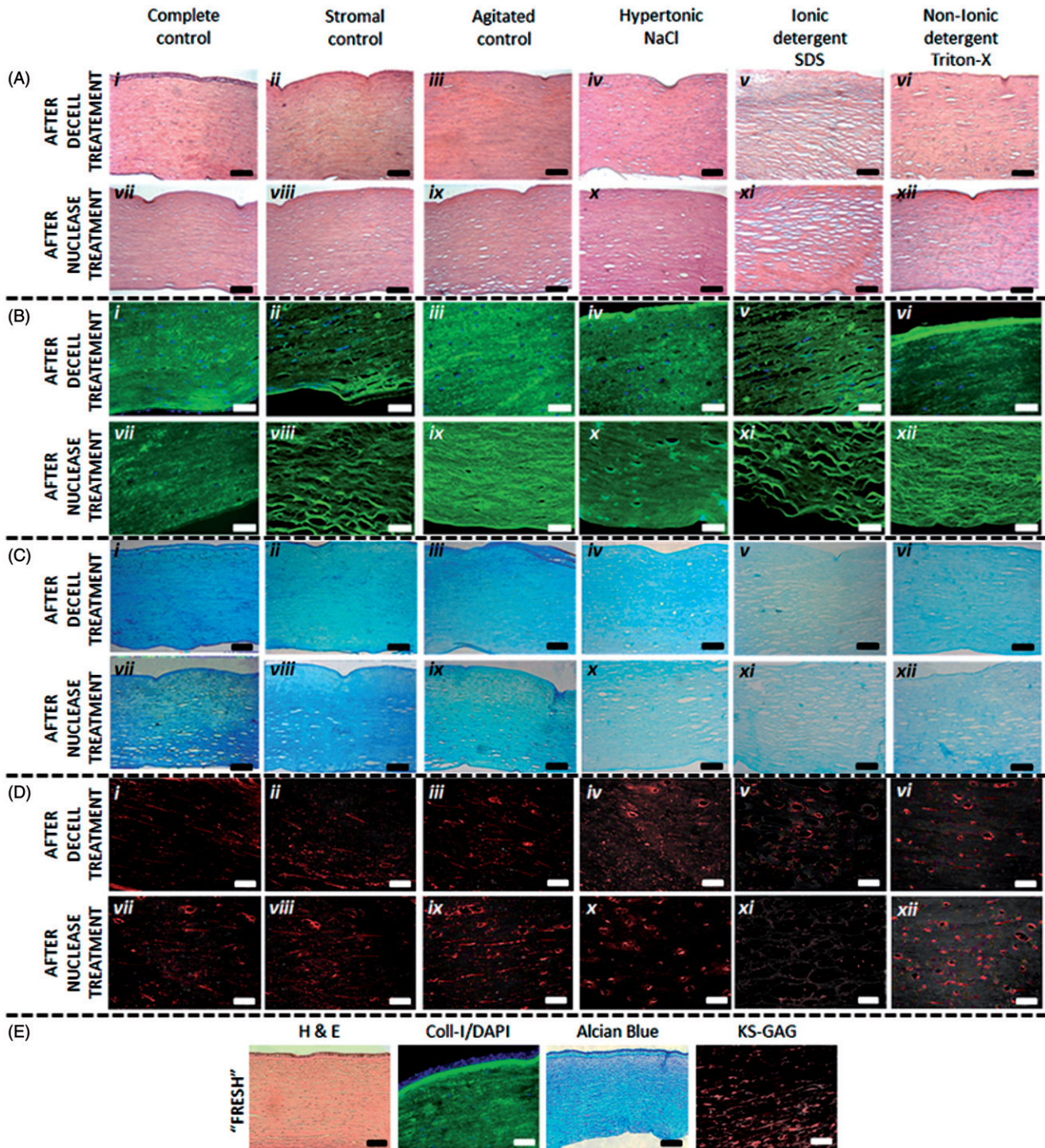


FIGURE 2 (A) Haematoxylin/Eosin staining of corneal sections after decellularization treatments (*i-vi*) and following an additional nuclease treatment (*vii-xii*); scale bar = 100 μ m. The images demonstrate the disruptive nature of SDS in particular on the corneal collagen architecture. (B) Collagen-I and DAPI staining of corneal sections following decellularization treatments (*i-vi*) and following an additional nuclease treatment (*vii-xii*), scale bar = 50 μ m. (C) Alcian blue staining of corneal sections after decellularization treatments (*i-vi*) and following an additional nuclease treatment (*vii-xii*); scale bar = 100 μ m. The images demonstrate a decrease in GAG content following decellularization treatments. (D) KS-GAG immunohistochemical staining demonstrates KS-GAG distribution in corneas following decellularization treatments (*i-vi*) and following an additional nuclease treatment (*vii-xii*), scale bar = 50 μ m. (E) Comparative staining of "freshly" dissected corneal tissue, demonstrating that submersion in PBS (complete control) does not have an effect on tissue structure, cellular and glycosaminoglycan content and distribution.

Following nuclease treatment all corneas, irrespective of the initial decellularization treatment, had significantly lower residual DNA ($p \leq 0.0001$) than non-nuclease treated corneas (Figure 3D). All

nuclease-treated corneas, with the exception of the agitated controls had significantly less residual DNA ($p \leq 0.01$) than the nuclease-treated complete controls (Figure 3C). Nuclease treatment was most successful

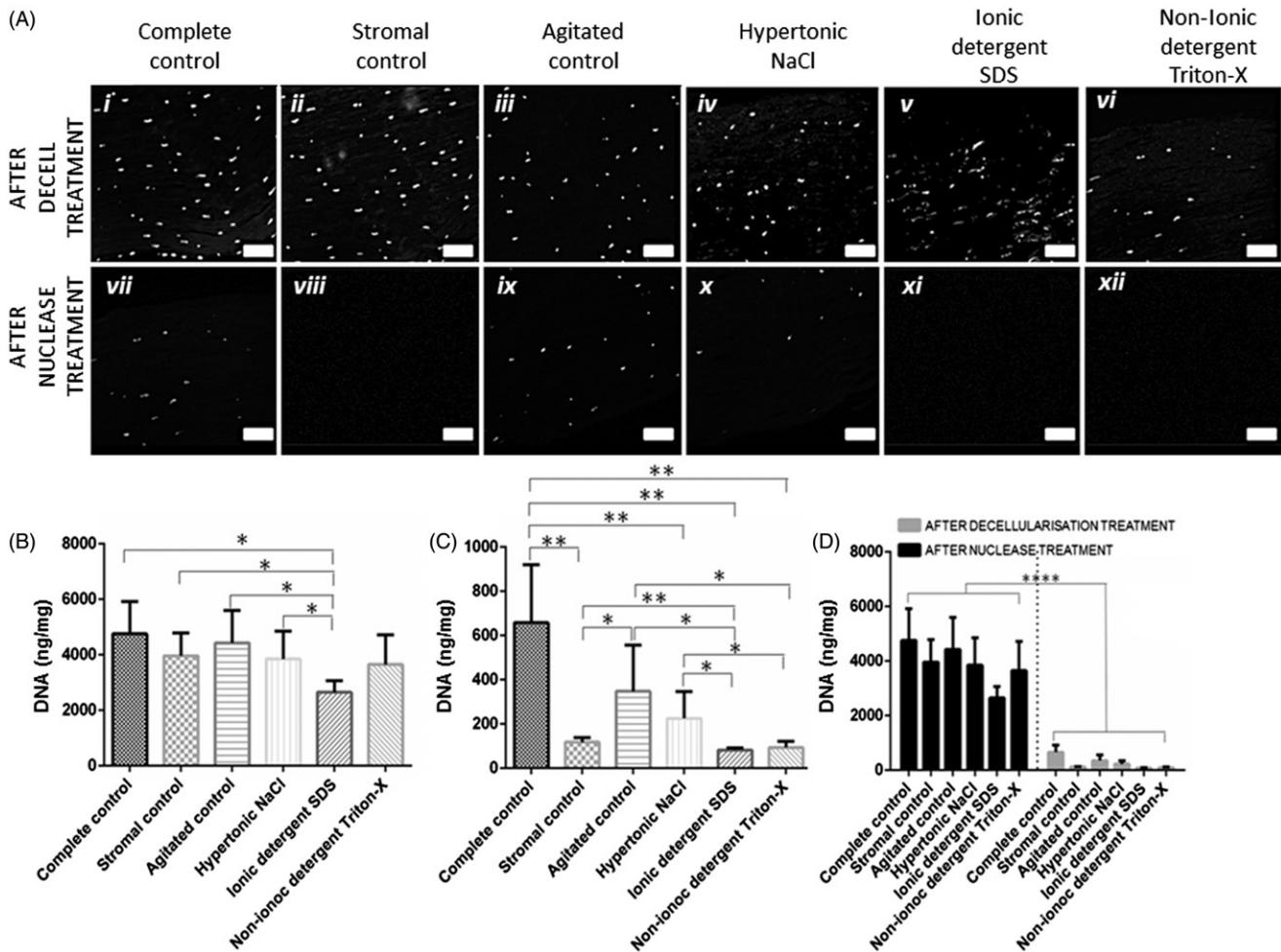


FIGURE 3 (A) DAPI staining of nuclear material demonstrated that initial decellularization treatments fail to completely remove nuclear material (*i–vi*), nuclease treated corneas were observed to have significantly less positive DAPI staining (*vii–xii*), scale bar = 50 μm. (B) Quantification of residual DNA following decellularization treatments. (C) Quantification of residual DNA following decellularization with an additional nuclease treatment. (D) A direct comparison of non-nuclease treated corneas versus nuclease treated corneas, *n* = 5. Data represented as the mean value ± the calculated SD. **p* ≤ 0.05, ***p* ≤ 0.01, ****p* ≤ 0.001.

in SDS (98.3% DNA removed) and Triton-X (98.0% DNA removed) decellularized corneas; both had significantly less DNA remaining than the stromal controls (*p* ≤ 0.01) and NaCl-treated corneas (*p* ≤ 0.05).

Collagen Quantification

The Sircol™ collagen assay revealed that the different decellularization procedures had no significant effect on collagen content compared to the control corneas (Figure 4A). All corneas had an average dry weight of 16.2 mg and a collagen dry weight of 11.5 mg, which equates to 70.8% collagen comprising the total dry weight of the cornea.

sGAG Content as a Marker of the Stripping Effects of Decellularization

The DMMB assay revealed that all decellularization treatments reduced sGAG content. The removal of the

epithelium and endothelium in the stromal controls and mechanical agitation alone had no significant effect on sGAG content (Figure 4B). sGAGs depletion was most apparent in SDS-treated corneas (>70% sGAGs removed), with the reduction in sGAGs being significantly greater compared to all controls (*p* ≤ 0.0001 compared to complete and stromal controls; *p* ≤ 0.001 compared to agitated controls); NaCl (*p* ≤ 0.05) and Triton-X-treated corneas (*p* ≤ 0.01). NaCl-treated corneas had the second greatest reduction in sGAGs compared to control corneas (*p* ≤ 0.001 compared to complete controls; *p* ≤ 0.01 compared to stromal and agitated controls), with >45% sGAG reduction. There was no significant difference when comparing sGAGs in NaCl corneas with Triton-X corneas. Triton-X corneas experienced approximately 40% depletion in sGAGs, which was significantly less than all control corneas (*p* ≤ 0.01). Although sGAG content in the stromal control, agitated control and Triton-X corneas appeared to be slightly lower following nuclease treatment, the differences were not significant.

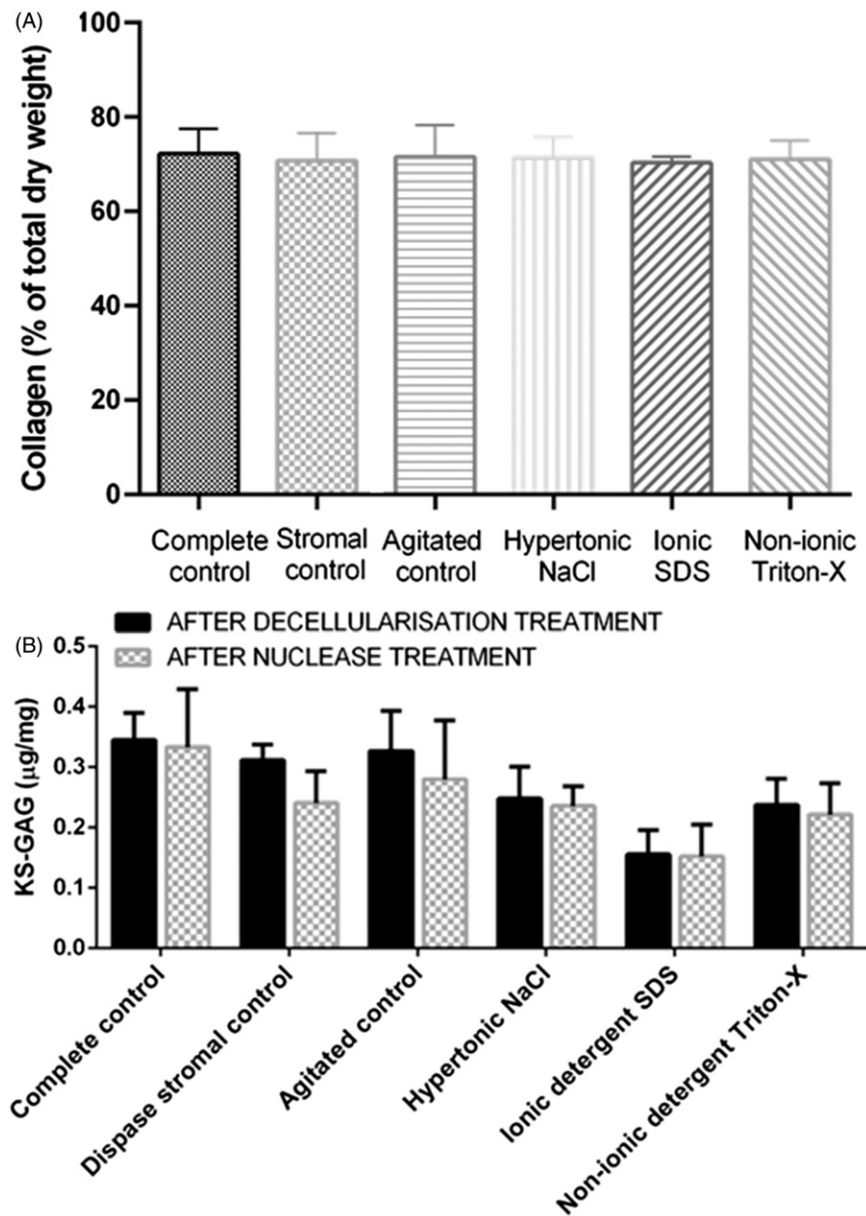


FIGURE 4 (A) Quantification of collagen content following decellularization with nucleases. The different decellularization protocols had no effect on collagen concentration. (B) Quantification of sGAG following initial decellularization treatments and decellularization with an additional nuclease treatment $n = 5$. Data represented as the mean value \pm the calculated SD. The additional nuclease treatment did not cause a significant reduction in s-GAG content.

Alcian blue histological staining validated the diminution in GAG content (Figure 2*Ci–xiii*), with a significant decrease in Alcian blue saturation in all decellularized corneas, irrespective of the treatment, compared to the complete, stromal and agitated control corneas (Figure 2*Ci–vi*). Alcian blue staining was least in SDS corneas (Figure 2*Cv*). There was no apparent effect on Alcian blue staining following treatment with nucleases (Figure 2*Cvii–xiii*).

Immunohistochemical staining of all control corneas demonstrated KS-GAGs distributed in thin bands running in parallel between the collagen fibers (Figure 2*Di–iii* and *Dvii–ix*). It was revealed in corneas treated with NaCl, SDS and Triton-X that not only was KS-GAG staining reduced, but the

distribution of the KS-GAGs was significantly disrupted (Figure 2*Div–vi* and *Dx–xviii*). Nuclease treatment had no apparent effect of KS-GAG staining.

Scaffold Biocompatibility

No cellular outgrowth from the corneal tissues onto the transwell inserts was observed. Cell proliferation was limited to the monolayer of CSC cultured in the companion plate. PrestoBlue™ analysis at day 0 revealed no significant difference in proliferation between groups (Figure 5). CSC cultured in the presence of 0.5% *w/v* SDS (negative controls) lysed within minutes, and no proliferation occurred.

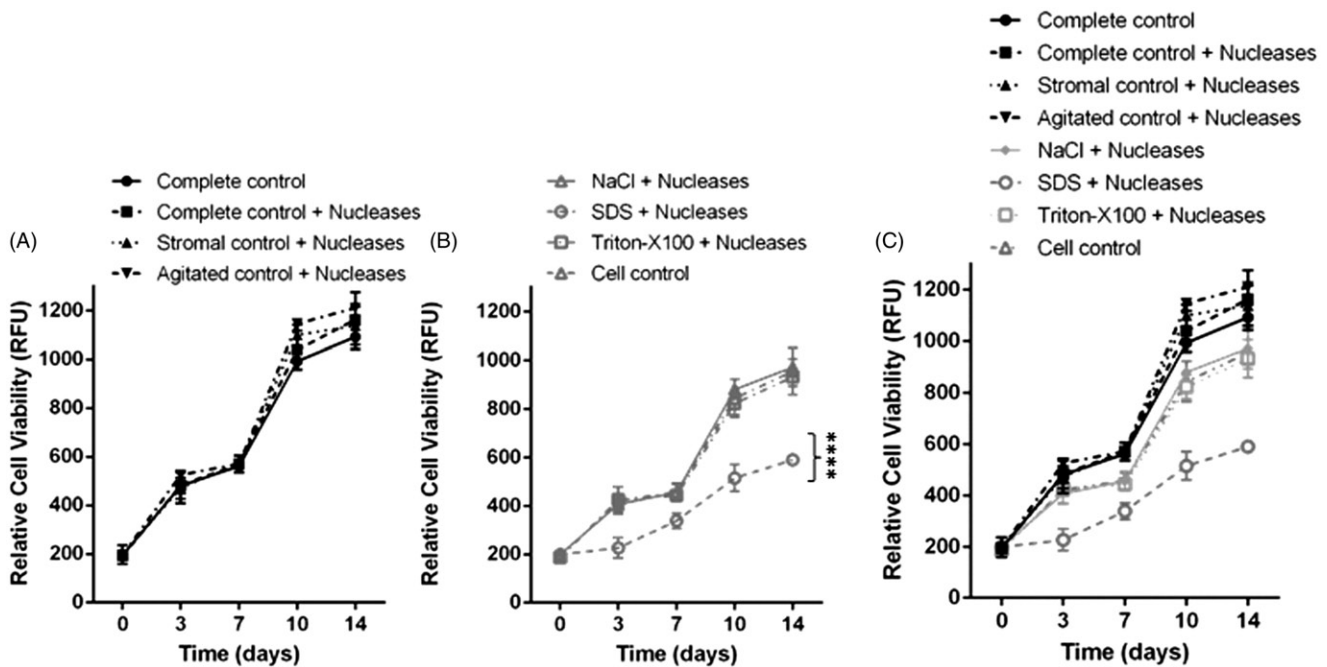


FIGURE 5 (A) Relative cell viability of corneal stromal cells cultured with control corneal tissues. All cells cultured with control corneal tissue (complete, stromal and agitated) proliferated at a greater rate than the control cells cultured without corneal tissue, although these differences were not significant. (B) Relative cell viability of corneal stromal cells cultured with decellularized corneal tissues. Cells cultured with corneal tissue decellularized with SDS proliferated significantly less compared to the NaCl and Triton-X decellularized tissues, and the cellular control, $p \leq 0.0001$. (C) Combined analysis of cell viability with both cells cultured with control and decellularized tissues displayed on the same graph $n = 5$. Data represented as the mean value \pm the calculated SD.

Following 3, 7, 10 and 14 days cells cultured with SDS-treated tissue with nucleases proliferated significantly less than all comparative samples ($p \leq 0.000$, Figure 5B). Following 3 days, there was no significant difference in proliferation when comparing the cellular controls to all control corneas and the NaCl and Triton-X with nuclease treated corneas. However, following 7 days CSC cultured with tissues treated with Triton-X with nucleases proliferated significantly less than CSC cultured with the complete control, complete control with nucleases, stromal control with nucleases and agitated control corneas ($p \leq 0.05$). There was no significant difference in proliferation when comparing CSC cultured with NaCl-treated corneas with nucleases, to Triton-X-treated corneas with nucleases or the cell control cultured without corneal tissue.

Following 10 days, proliferation was significantly lower in cells cultured with tissues that had been decellularized using NaCl with nucleases, Triton-X with nucleases and the cellular control, when compared to CSC cultured with the complete control tissue, complete control with nucleases, stromal control with nucleases and the agitated control with nucleases. This trend was repeated at 14 days. In general, CSC cultured with control tissues, proliferated more than CSC cultured without corneal tissue and the decellularized tissue. Corneas treated with SDS with nucleases had the most antagonistic effect on proliferation.

DISCUSSION

The principal aim of any decellularization procedure is to reduce the likelihood of host rejection or immunological response upon transplantation, while maintaining the structural integrity and functional properties of the ECM.^{29,31,35,36} Often decellularization techniques aim to completely eradicate cellular and antigen material, including lipid membranes, membrane associated antigens and soluble proteins.^{14,30,37} However, such protocols inevitably cause tissue disruption and stripping of intrinsic biological cues. Likewise, techniques which maintain the ECM ultrastructure are likely to leave cellular artifacts and residual antigen molecules.

From a manufacturing point of view, simple protocols with fewer steps and minimal reagent use are desirable. Maintenance of tissue architecture, protein and GAG content is particularly important to decellularized tissues, since it is the structure that is responsible for corneal transparency and functionality.

Corneal Transparency, Light Transmittance and Structural Integrity

To have sufficient functionality, a decellularized cornea should ideally have low light absorption and

scattering in the visible region, while having acceptable refractive power.¹⁴ *In vivo* corneal transparency depends upon highly complex levels of organization and regular spatial ordering of the thin collagen fibrils within the stroma.^{38–40} The cornea is unique since nanoscale tissue disruption results in macroscopic changes, ultimately affecting transparency and light transmission. Thus, macroscopic evaluation following decellularization is a rudimentary method of determining if structural disruption has occurred.

The structure and composition of a biomaterial are as important in cell signaling as growth factors, cytokines and other mediators.³³ Structural changes following decellularization, including defects and voids within the matrix lead to structural compromise,⁴¹ responsible for poor long-term performance following implantation.³⁷ NaCl decellularized corneas yielded the most transparent tissues with least stromal disruption, in agreement with previous studies.²⁸ The exact mechanism whereby the osmotic agent NaCl decellularizes is not fully understood, however Gilbert *et al.* suggested that NaCl induces osmotic shock, triggering cell rupture within the tissue.³⁰ An alternative hypothesis proposes that Na and Cl ions capable of crossing cellular membranes extract water from cells, modifying cell volume, thus altering the macromolecular content, inducing cell death.⁴²

Non-ionic detergents disrupt lipid–lipid and lipid–protein interactions while leaving protein–protein interactions intact; they are generally non-denaturing, thus remaining proteins following Triton-X treatment should retain functional conformation.⁴³ Although reduced transparency and collagen disruption was observed in Triton-X treated corneas, it was not to the extent of SDS-treated corneas. Ionic detergents, including SDS, solubilize both cytoplasmic and nuclear cell membranes, damaging collagen³⁰ and denature proteins by disrupting protein–protein interactions.⁴³ As a result, SDS-treated corneas had the greatest loss of transparency with most ECM disruption compared to all other treatments, in agreement with other studies.^{22,28} This may affect the mechanical integrity of the tissue as demonstrated by Du *et al.*¹⁴ due to a denaturation of the collagen triple helix, or loss of macromolecular substances such as glycoproteins³⁷; ultimately affecting the tissue's ability to withstand surgical manipulation including suturing.

Interestingly, the stromal controls treated with Dispase to remove the epithelium and endothelium experienced reduced transparency. This may be due to the removal of the epithelium and endothelium damaging the basement membrane and Descemet's membrane respectively. However, the agitated controls did not experience reduced transparency, despite the epithelium and endothelium being absent. Thus, prolonged mechanical agitation alone may negate the need for the use of Dispase.

Irrespective of the decellularization treatment, nuclease treatments caused a further loss of transparency and additional structural disruption. Earlier studies reported a severe distortion of the collagen structure following nuclease treatments.²² Although the effect was not severe, structural distortion may have been caused by the hypotonic nature of the nuclease solutions, causing remaining cells to swell and lyse, resulting in the voids observed in the collagen structure.

Previous studies have demonstrated a “restoration” of corneal transparency following submersion in glycerol.²³ The mechanism whereby glycerol causes optical clearing is not fully understood, although transmission electron microscopy and polarized light microscopy studies have revealed that glycerol causes an unraveling, dissociation and loss of organization in the collagen fibril structure, although this is reversible upon submersion in PBS.⁴⁴ Scanning electron microscopy and optical coherence tomography analysis have revealed that glycerol reduces light scattering and causes structural modifications including increased pore sizes.⁴⁵ Thus, glycerol may mask structural damage as a result of the decellularization procedure, while also causing additional disorganization to the collagen structure. Therefore, glycerol was not included in this study.

Residual DNA

Extraction of residual cellular components is believed to minimize immunologically induced responses that lead to graft failure.^{14,46} Components of dead cells (cytosol, cell membranes, organelles and cytoskeleton) can also activate innate and acquired immune responses resulting in rejection^{46,47}; although it has been suggested a “threshold” amount of material is required to promote adverse remodeling responses following implantation.⁴⁷ Intracellular cytoplasmic protein and membrane components are likely to be retained within the tissue alongside residual DNA,⁴⁷ although decellularizing agents may alter residual cell products so they no longer stimulate adverse host responses.

Detergent use alone has been reported to be ineffective in eradicating cellular material from the cornea,¹⁴ which corresponds with our observations, as high amounts of DNA were detected following all initial decellularization treatments. SDS was most effective in removing cellular components, in agreement with previous studies¹⁴; as a result of collagen lattice disruption and increased interfibrillar spacing, leading to an increased surface area and porosity, thus allowing more cellular material to be released. Conversely, the relative conservation of the dense collagen network following all other decellularization treatments, although may have led to cell lysis and

apoptosis, did not sufficiently allow DNA release from the tissue.

Nucleases including endonucleases utilized in this study, catalyze the hydrolysis of interior bonds in the ribonucleotide or deoxyribonucleotide chains; cleavage mid-sequence leads to DNA fragmentation and degradation³⁰ enabling easier removal from the tissue. Nuclease treatment significantly reduced DNA, although was more successful in corneas pre-treated with decellularizing agents. This result is rational since the ECM needs to be adequately disrupted to allow cells exposure to nucleases, while providing a path for removal of cellular material.³⁰ Stromal controls had significantly lower DNA following nuclease treatment, potentially due to the removal of the epithelium and endothelium disrupting/damaging the barrier function of the basement membrane and/or the Descemet's membrane, allowing a higher efficacy of DNA removal following nuclease cleavage.

Collagen and sGAG Content as a Marker of the Stripping Effects of Decellularization Protocols

The effect of cell extraction on corneal ECM proteins has not been studied extensively.¹⁴ The majority of the stroma is comprised of collagen I, V, VI and XII, along with dermatan sulfate proteoglycan decorin and keratan sulfate proteoglycans lumican, keratocan, osteoglycin (mimican)^{48,49} and small amounts of heparin⁵⁰ forming the ground substances of the stroma, responsible for the spatial distribution and organization of the collagen fibrils,^{38,51} assembly and fibrillogenesis.⁵⁰ GAGs also bind growth factors and cytokines, promote water retention and contribute to the gel properties of the ECM.⁵² Thus, any alteration/reduction in GAG-content in decellularized corneas may affect the tissue bioactivity.

Previous studies on numerous tissues have demonstrated that despite structural disruption and reduced cellular and GAG content, collagen content is not affected by decellularizing reagents.^{33,53–55} Quantification of collagen following the different decellularization protocols agreed with these studies.

It was observed in control corneas that KS-GAG expression manifested as thin, fibrillar streaks between collagen fibers, as previously observed.⁵⁰ Following decellularization, KS-GAG expression was reduced as previously reported.³⁶ Perhaps more importantly, remaining KS-GAGs distribution was disrupted.

Mendoza-Novelo et al. suggested that sGAG removal is influenced not only by the type of decellularization reagent used, but also the swelling behavior of the tissue.³⁶ Since SDS-treated corneas experienced greatest collagen disruption, interfibrillar spacing and ultimately increased swelling, observed

subjectively, more GAGs could be released compared to Triton-X-treated tissues. Similar results were observed³³ whereby tissues treated with mild non-ionic detergents removed free-GAGs, whereas those treated with strong ionic detergents caused additional dissociation of proteoglycans bound to the collagen fibrils.

Scaffold Biocompatibility

Proliferation studies were utilized as a rudimentary indicator of the biocompatibility of the decellularized scaffolds. All cells cultured with control tissues proliferated more than cells cultured with decellularized tissue. Improved cell growth may have occurred for a number of reasons: (i) the intrinsic, biological cues including GAGs, remaining within the structure of untreated tissues had a favorable stimulatory effect on proliferation; a hypothesis supported by previous work by Gratzer et al.⁵⁶ It was observed that cells cultured in the presence of decellularized tissues, whereby structural disruption and GAGs had diminished, proliferation was significantly reduced. (ii) Residual decellularizing agents were detrimentally effecting cell growth and proliferation. SDS in particular, is notoriously difficult to eradicate following decellularization and residual detergent is thought to have cytotoxic effects as it leaches from the tissue.^{37,57}

Conversely, cellular material remaining in control tissues may have detrimentally affected proliferation. Extensive studies have demonstrated that the healthy corneal stromal cell phenotype, the keratocyte, is quiescent.^{34,58–66} A proliferative CSC, the fibroblast or myofibroblast, would indicate an inflammatory response resulting in an activation of the CSC into an injury phenotype.^{34,58,61,62,67–70} However, we believe this effect is superseded by the fact that cells were cultured in serum-containing media, known to initiate CSC activation and proliferation.^{34,48,64} In this instance, reduced proliferation was indicative of an ineffective decellularization procedure.

CONCLUSION

The ability to utilize, reprocess and regenerate tissue "unsuitable" for transplantation allows us to salvage valuable tissue. Reprocessing tissue has the potential to have considerable impact on addressing donor shortages. Recently, standard corneal treatments have shifted from complete transplantation to procedures that replace the diseased or injured area.²² Decellularized tissues may potentially be utilized in partial-thickness lamellar keratoplasty procedures in patients who have stromal opacities, while retaining a healthy endothelium. Patients would benefit directly by accessing greater numbers of corneal grafts, while

health authorities would fulfill their responsibility to deliver effective corneal reconstruction to alleviate corneal blindness.

Ultimately, due to the way cells are embedded within tissue ECM, especially dense corneal tissue, it is extremely unlikely that any decellularization technique will successfully remove 100% of cellular components.⁴⁷ Most commercially available “decellularized” scaffolds contain small amounts of remnant DNA.⁴⁷ However, even the most effective decellularization method is unsuitable if it prevents subsequent cellular repopulation³³ due to matrix disruption and residual chemicals. Since the stroma is sparsely populated with “immune privileged” keratocytes,^{11,12} complete eradication of cellular material may not necessarily be most appropriate, and may provoke an immune response in the resulting tissue due to the dispersion and incomplete removal of keratocyte debris.

The decellularization protocol may be harmful to the function of the biomaterial if structural integrity is greatly compromised.³³ This may warrant a change from “traditional”, often laborious, decellularization procedures reliant upon extensive use of reagents and washing steps, which ultimately are not up-scalable from a manufacturing point of view. Since the proliferation studies demonstrated that residual CSC did not adversely affect proliferation; and tissue rejection following corneal allografting is predominantly caused by epithelial and endothelial rejection,⁷¹ it may be plausible to simply remove the epithelium and endothelium. Since agitation alone was sufficient in removing these layers, with minimal disruption to the stroma, transparency and GAG content, thus maintaining tissue functionality with an intact basement and Descemet’s membrane; agitation alone will be further investigated as a potential technique for recycling corneal tissue. The remaining “immune privileged” keratocytes would remain intact, with no fragmented DNA, residual artifacts or antigen molecules. This technique would also negate the need for further studies to assess the removal of residual chemicals from the tissue as they may have cytotoxic effects, while also inhibiting cell adhesion, migration and proliferation,⁴¹ leading to tissue rejection.²² Although the complete removal of any antibiotic/antimycotic agents needs to be ensured so that the construct is not considered a medical device by regulatory bodies.

Additional transmission electron microscopy (TEM) would be beneficial in analyzing the ultrastructure of the corneal stroma following decellularization. This would allow for the orientation of collagen fibrils and disruption to the highly organized architecture following decellularization to be examined and compared to the native cornea. The extent to which the typical orthogonal arrangement of fibril bands and tightly packed lamellae is disrupted following

decellularization could be used to determine if such changes have an impact on scaffold biocompatibility and remodeling following recellularization.

Although there are still many challenges to address prior to clinical translation, the “recycling” of unsuitable tissues still represents a promising alternative to cadaveric tissue. However, in order to progress, we may need to take a step back to establish a “decellularization” criterion; which should balance effective removal of immune reactive material with maintenance of tissue functionality; along with the development of appropriate, systematic and standardized screening protocols.

ACKNOWLEDGMENTS

Invaluable technical assistance and expertise from Denise Mclean, in the Advanced Microscopy Unit (School of Life Sciences, University of Nottingham), is very much appreciated.

DECLARATION OF INTEREST

The authors report no conflict of interest. The authors alone are responsible for the content and writing of the manuscript. Funding from EPSRC Engineering, Tissue Engineering and Regenerative Medicine (E-TERM), grant number: EP/I017801/1; is gratefully acknowledged.

REFERENCES

- Whitcher JP, Srinivasan M, Upadhyay MP. Corneal blindness: a global perspective. *Bull World Health Organ* 2001; 79:214–221.
- Huang Y-X, Li Q-H. An active artificial cornea with the function of inducing new corneal tissue generation in vivo – a new approach to corneal tissue engineering. *Biomed Mater* 2007;2:121–125.
- Carlsson DJ, Li F, Shimmura S, Griffith M. Bioengineered corneas: how close are we? *Curr Opin Ophthalmol* 2003;14: 192–197.
- Chirila TV, Hicks CR, Dalton PD, Vijayasekaran S, Lou X, Hong Y, et al. Artificial cornea. *Prog Polym Sci* 1998;23: 447–473.
- Oliva MS, Schottman T, Gulati M. Turning the tide of corneal blindness. *Indian J Ophthalmol* 2012;60:423–427.
- WHO. Prevention of blindness and visual impairment: priority eye diseases: corneal opacities 2014. Available from: <http://www.who.int/blindness/causes/priority/en/index8.html> [accessed 24 Oct 2014].
- Hara H, Cooper DK. Xenotransplantation – the future of corneal transplantation? *Cornea* 2011;30:371–378.
- Shao Y, Yu Y, Pei CG, Zhou Q, Liu QP, Tan G, et al. Evaluation of novel decellularizing corneal stroma for cornea tissue engineering applications. *Int J Ophthalmol* 2012;5:415–418.
- Stevenson W, Cheng S-F, Emami-Naeini P, Hua J, Paschalis EI, Dana R, et al. Gamma-irradiation reduces the

- allogenicity of donor corneas. *Invest Ophthalmol Vis Sci* 2012;53:7151–7158.
10. Le Discorde M, Moreau P, Sabatier P, Legeais J-M, Carosella ED. Expression of HLA-G in human cornea, an immune-privileged tissue. *Hum Immunol* 2003;64:1039–1044.
 11. Wilson SE, Liu JJ, Mohan RR. Stromal-epithelial interactions in the cornea. *Prog Retin Eye Res* 1999;18:293–309.
 12. Vij N, Roberts L, Joyce S, Chakravarti S. Lumican suppresses cell proliferation and aids Fas–Fas ligand mediated apoptosis: implications in the cornea. *Exp Eye Res* 2004;78:957–971.
 13. Khodadoust AA. The allograft rejection reaction: the leading cause of late failure of clinical corneal grafts. In: Porter R, Knight J, editors. *Ciba Foundation Symposium 15 – Corneal Graft Failure*. Amsterdam: John Wiley & Sons, Ltd; 2008. pp 151–167.
 14. Du L, Wu X, Pang K, Yang Y. Histological evaluation and biomechanical characterisation of an acellular porcine cornea scaffold. *Br J Ophthalmol* 2011;95:410–414.
 15. NHSBT. Organ Donation and Transplantation Activity Report 2013/14 2015. Available from: https://nhsbtmediaservices.blob.core.windows.net/organ-donation-assets/pdfs/activity_report_2013_14.pdf [accessed 18 Feb 2015].
 16. Shafiq MA, Gemeinhart RA, Yue BY, Djalilian AR. Decellularized human cornea for reconstructing the corneal epithelium and anterior stroma. *Tissue Eng Part C Methods* 2012;18:340–348.
 17. Gonzalez Andrades M, Martin-Piedra MA, Alfonso C, Carriel V, Crespo PV, Alaminos M, et al. Generation of a complete anterior lamellar human cornea using decellularized stromas. *J Tissue Eng Regen Med* 2012;6:138.
 18. Keenan TDL, Carley F, Yeates D, Jones MNA, Rushton S, Goldacre MJ. Trends in corneal graft surgery in the UK. *Br J Ophthalmol* 2011;95:468–472.
 19. Du L, Wu X. Development and characterization of a full-thickness acellular porcine cornea matrix for tissue engineering. *Artif Organs* 2011;35:691–705.
 20. Gonzalez-Andrades M, de la Cruz Cardona J, Maria Ionescu A, Campos A, del Mar Perez M, Alaminos M. Generation of bioengineered corneas with decellularized xenografts and human keratocytes. *Invest Ophthalmol Vis Sci* 2011;52:215–222.
 21. Hashimoto Y, Funamoto S, Sasaki S, Honda T, Hattori S, Nam K, et al. Preparation and characterization of decellularized cornea using high-hydrostatic pressurization for corneal tissue engineering. *Biomaterials* 2010;31:3941–3948.
 22. Oh JY, Kim MK, Lee HJ, Ko JH, Wee WR, Lee JH. Processing porcine cornea for biomedical applications. *Tissue Eng Part C Methods* 2009;15:635–645.
 23. Pang K, Du L, Wu X. A rabbit anterior cornea replacement derived from acellular porcine cornea matrix, epithelial cells and keratocytes. *Biomaterials* 2010;31:7257–7265.
 24. Sasaki S, Funamoto S, Hashimoto Y, Kimura T, Honda T, Hattori S, et al. In vivo evaluation of a novel scaffold for artificial corneas prepared by using ultrahigh hydrostatic pressure to decellularize porcine corneas. *Mol Vis* 2009;15:2022–2028.
 25. Wu Z, Zhou Y, Li N, Huang M, Duan H, Ge J, et al. The use of phospholipase A(2) to prepare acellular porcine corneal stroma as a tissue engineering scaffold. *Biomaterials* 2009;30:3513–3522.
 26. Yoeruek E, Bayyoud T, Maurus C, Hofmann J, Spitzer MS, Bartz-Schmidt K-U, et al. Decellularization of porcine corneas and repopulation with human corneal cells for tissue-engineered xenografts. *Acta Ophthalmol* 2012;90:125–131.
 27. Boneva RS, Folks TM. Xenotransplantation and risks of zoonotic infections. *Ann Med* 2004;36:504–517.
 28. Gonzalez-Andrades M, de la Cruz Cardona J, Ionescu AM, Campos A, Del Mar Perez M, Alaminos M. Generation of bioengineered corneas with decellularized xenografts and human keratocytes. *Invest Ophthalmol Vis Sci* 2011;52:215–222.
 29. Crapo PM, Gilbert TW, Badylak SF. An overview of tissue and whole organ decellularization processes. *Biomaterials* 2011;32:3233–3243.
 30. Gilbert TW, Sellaro TL, Badylak SF. Decellularization of tissues and organs. *Biomaterials* 2006;27:3675–3683.
 31. Lynch AP, Ahearne M. Strategies for developing decellularized corneal scaffolds. *Exp Eye Res* 2012;108C:42–47.
 32. Wilson SL, Sidney LE, Dunphy SE, Rose JB, Hopkinson A. Keeping an eye on decellularized corneas: a review of methods, characterization and applications. *J Funct Biomater* 2013;4:114–161.
 33. Vavken P, Joshi S, Murray MM. TRITON-X is most effective among three decellularization agents for ACL tissue engineering. *J Orthop Res* 2009;27:1612–1618.
 34. Wilson SL, Yang Y, El Haj AJ. Corneal stromal cell plasticity: in vitro regulation of cell phenotype through cell-cell interactions in a three-dimensional model. *Tissue Eng Part A* 2014;20:225–238.
 35. Liao J, Joyce EM, Sacks MS. Effects of decellularization on the mechanical and structural properties of the porcine aortic valve leaflet. *Biomaterials* 2008;29:1065–1074.
 36. Mendoza-Novelo B, Avila EE, Cauich-Rodríguez JV, Jorge-Herrero E, Rojo FJ, Guinea GV, et al. Decellularization of pericardial tissue and its impact on tensile viscoelasticity and glycosaminoglycan content. *Acta Biomater* 2011;7:1241–1248.
 37. Courtman DW, Pereira CA, Kashef V, McComb D, Lee JM, Wilson GJ. Development of a pericardial acellular matrix biomaterial: biochemical and mechanical effects of cell extraction. *J Biomed Mater Res* 1994;28:655–666.
 38. Fullwood NJ. Collagen fibril orientation and corneal curvature. *Structure* 2004;12:169–170.
 39. Meek KM, Boote C. The use of X-ray scattering techniques to quantify the orientation and distribution of collagen in the corneal stroma. *Prog Retin Eye Res* 2009;28:369–392.
 40. Kim A, Zhou C, Lakshman N, Petrol WM. Corneal stromal cells use both high- and low-tractility migration mechanisms in 3-D collagen matrices. *Exp Eye Res* 2012;318:741–752.
 41. Ketchedjian A, Jones AL, Krueger P, Robinson E, Crouch K, Wolfenbarger Jr L, et al. Recellularization of decellularized allograft scaffolds in ovine great vessel reconstructions. *Ann Thorac Surg* 2005;79:888–896.
 42. Richter K, Nessling M, Lichter P. Experimental evidence for the influence of molecular crowding on nuclear architecture. *J Cell Sci* 2007;120:1673–1680.
 43. Seddon AM, Curnow P, Booth PJ. Membrane proteins, lipids and detergents: not just a soap opera. *Biochim Biophys Acta Biomembranes* 2004;1666:105–117.
 44. Yeh AT, Choi B, Nelson JS, Tromberg BJ. Reversible dissociation of collagen in tissues. *J Invest Dermatol* 2003;121:1332–1335.
 45. Zhao S, Shen Z, Wang J, Li X, Zeng Y, Wang B, et al. Glycerol-mediated nanostructure modification leading to improved transparency of porous polymeric scaffolds for high performance 3D cell imaging. *Biomacromolecules* 2014;15:2521–2531.
 46. Böer U, Lohrenz A, Klingenberg M, Pich A, Haverich A, Wilhelmi M. The effect of detergent-based decellularization procedures on cellular proteins and immunogenicity in equine carotid artery grafts. *Biomaterials* 2011;32:9730–9737.

47. Gilbert TW, Freund JM, Badylak SF. Quantification of DNA in biologic scaffold materials. *J Surg Res* 2009;152:135–139.
48. Carlson EC, Wang IJ, Liu CY, Brannan P, Kao CWC, Kao WWY. Altered KSPG expression by keratocytes following corneal injury. *Mol Vis* 2003;9:615–623.
49. Bron AJ. The architecture of the corneal stroma. *Br J Ophthalmol* 2001;85:379–381.
50. Akhtar S, Kerr BC, Hayes AJ, Hughes CE, Meek KM, Caterson B. Immunohistochemical localization of keratan sulfate proteoglycans in cornea, sclera, and limbus using a keratanase-generated neopeptide monoclonal antibody. *Invest Ophthalmol Vis Sci* 2008;49:2424–2431.
51. Meek KM, Boote C. The organization of collagen in the corneal stroma. *Exp Eye Res* 2004;78:503–512.
52. Badylak SF. Xenogeneic extracellular matrix as a scaffold for tissue reconstruction. *Transpl Immunol* 2004;12:367–377.
53. Xu H, Xu B, Yang Q, Li X, Ma X, Xia Q, et al. Comparison of decellularization protocols for preparing a decellularized porcine annulus fibrosus scaffold. *PLoS One* 2014;9:e86723.
54. Youngstrom DW, Barrett JG, Jose RR, Kaplan DL. Functional characterization of detergent-decellularized equine tendon extracellular matrix for tissue engineering applications. *PLoS One* 2013;8:e64151.
55. Elder BD, Kim DH, Athanasiou KA. Developing an articular cartilage decellularization process toward facet joint cartilage replacement. *Neurosurgery* 2010;66:722–727.
56. Gratzner PF, Harrison RD, Woods T. Matrix alteration and not residual sodium dodecyl sulfate cytotoxicity affects the cellular repopulation of a decellularized matrix. *Tissue Eng* 2006;12:2975–2983.
57. Caamano S, Shiori A, Strauss SH, Orton EC. Does sodium dodecyl sulfate wash out of detergent-treated bovine pericardium at cytotoxic concentrations? *J Heart Valv Dis* 2009;18:101–105.
58. Wilson SL, Wimpenny I, Ahearne M, Rauz S, El Haj AJ, Yang Y. Chemical and topographical effects on cell differentiation and matrix elasticity in a corneal stromal layer model. *Adv Funct Mater* 2012;22:3641–3649.
59. Ahearne M, Wilson SL, Liu K-K, Rauz S, El Haj AJ, Yang Y. Influence of cell and collagen concentration on the cell-matrix mechanical relationship in a corneal stroma wound healing model. *Exp Eye Res* 2010;91:584–591.
60. Wilson SL, El Haj AJ, Yang Y. Control of scar tissue formation in the cornea: strategies in clinical and corneal tissue engineering. *J Func Biomater* 2012;3:642–687.
61. Fini ME. Keratocyte and fibroblast phenotypes in the repairing cornea. *Prog Retin Eye Res* 1999;18:529–551.
62. Jester JV, Ho-Chang J. Modulation of cultured corneal keratocyte phenotype by growth factors/cytokines control in vitro contractility and extracellular matrix contraction. *Exp Eye Res* 2003;77:581–592.
63. Builles N, Bechetoille N, Justin V, Ducerf A, Auxenfans C, Burillon C, et al. Development of an optimised culture medium for keratocytes in monolayer. *Bio-Med Mater Eng* 2006;16:95–104.
64. Berryhill BL, Kader R, Kane B, Birk DE, Feng J, Hassell JR. Partial restoration of the keratocyte phenotype to bovine keratocytes made fibroblastic by serum. *Invest Ophthalmol Vis Sci* 2002;43:3416–3421.
65. Pei Y, Reins RY, McDermott AM. Aldehyde dehydrogenase (ALDH) 3A1 expression by the human keratocyte and its repair phenotypes. *Exp Eye Res* 2006;83:1063–1073.
66. Pei Y, Sherry DM, McDermott AM. Thy-1 distinguishes human corneal fibroblasts and myofibroblasts from keratocytes. *Exp Eye Res* 2004;79:705–712.
67. Matsuda S, Hisama M, Shibayama H, Itou N, Iwaki M. Application of the reconstructed rabbit corneal epithelium model to assess the in vitro eye irritancy test of chemicals. *Yakugaku Zasshi* 2009;129:1113–1120.
68. Garana R, Petroll W, Chen W, Herman I, Barry P, Andrews P, et al. Radial keratotomy. II. Role of the myofibroblast in corneal wound contraction. *Invest Ophthalmol Vis Sci* 1992;33:3271–3282.
69. Beales MP, Funderburgh JL, Jester JV, Hassell JR. Proteoglycan synthesis by bovine keratocytes and corneal fibroblasts: maintenance of the keratocyte phenotype in culture. *Invest Ophthalmol Vis Sci* 1999;40:1658–1663.
70. Funderburgh JL, Mann MM, Funderburgh ML. Keratocyte phenotype mediates proteoglycan structure: a role for fibroblasts in corneal fibrosis. *J Biol Chem* 2003;278:45629–45637.
71. Keenan TL, Jones MA, Rushton S, Carley FM, National Health Service B, Transplant Ocular Tissue Advisory G, et al. Trends in the indications for corneal graft surgery in the united kingdom: 1999 through 2009. *Arch Ophthalmol* 2012;130:621–628.